

## Supporting Information

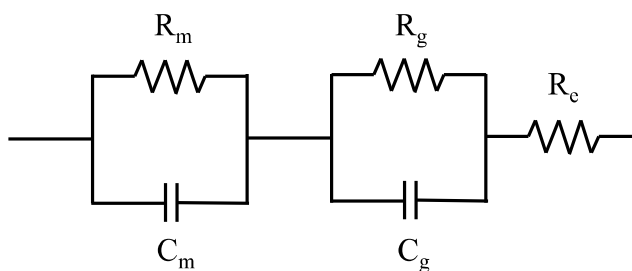
Charging the Quantum Capacitance of Graphene with a Single Biological Ion Channel

*Yung Yu Wang<sup>†</sup>, Ted D. Pham<sup>††</sup>, Katayoun Zand<sup>‡</sup>, Jinfeng Li<sup>†††</sup>, and Peter J. Burke<sup>‡</sup>*

<sup>†</sup>Department of Chemical Engineering and Materials Science, <sup>††</sup>Department of Biomedical Engineering, <sup>†††</sup>Department of Physics and <sup>‡</sup>Department of Electrical Engineering and Computer Science, University of California, Irvine, Irvine, California 92697, United States.

Supporting Information 1: The expanded circuit diagram

The simplified circuit diagram (Figure 3b) contains all the essential components, but here we discuss the additional components, determine their values, and discuss why they do not significantly change the conclusions of the manuscript. Figure S1 shows a more complete equivalent circuit for our device which we now discuss.



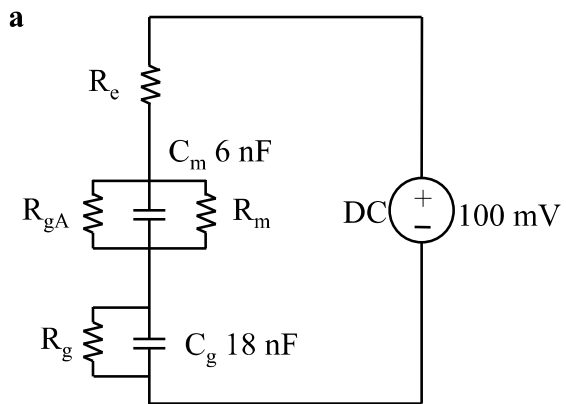
$$Z = R_e + \frac{R_m(1 + j\omega R_g C_g) + R_s(1 + j\omega R_m C_m)}{(1 + j\omega R_g C_g)(1 + j\omega R_m C_m)}$$

Figure S1. Equivalent circuit model with two time constants.  $R_e$  is the electrolyte resistance,  $R_g$  is the charge transfer resistance of the graphene/electrolyte interface,  $C_g$  stands for the double

layer capacitance of the graphene/electrolyte interface in series with the quantum capacitance of the graphene sheet.  $R_m$  and  $C_m$  are the lipid layer resistance and capacitance.

The electrolyte-graphene Faradaic current is expected to be small since we do not have a redox active species, and the applied potentials are within the window of voltage where the water is not electrochemically active. Based on the measured DC current from graphene to solution in the absence of SLBs, we estimate the value of  $R_g$  in the circuit to be  $\sim 10 \text{ M}\Omega$ . After addition of the lipid bilayer, this rises to  $\sim 500 \text{ M}\Omega$ . Thus we estimate the bilayer membrane resistance  $R_m$  to be  $\sim 0.5 \text{ G}\Omega$ . Both of these resistances were determined by dc measurements (see main text), but also verified by electrochemical impedance spectroscopy, discussed below. From a circuit point of view this resistance is large enough that it does not perturb the currents significantly. The electrolyte, reference electrode and contact resistances all shown by the series resistance ( $R_e = 20 \text{ k}\Omega$ ), small enough that it does not significantly perturb the currents flowing through the gA channel ( $R_{gA} = 100 \text{ G}\Omega$ ).

The circuit diagram is simulated in a circuit simulator. It is assumed the gramicidin channel has a resistance of  $100 \text{ G}\Omega$  and remains open for 0.1 seconds. The simulation result of the current step is measured by the patch clamp amplifier (Figure S2b). The result is similar to our ion channel measurements (Figure 3f and 3i) and shows the leakage resistors do not affect the behavior of the system significantly.



**b** Current through the patch clamp amplifier

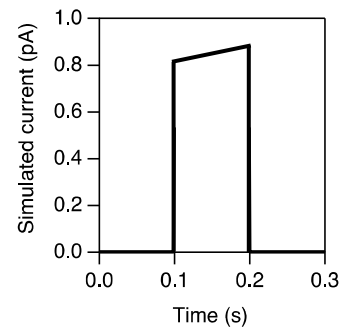


Figure S2. (a) Circuit diagram of graphene-SLBs. (b) Simulation result showing the current sensed through the patch clamp.

## Supporting Information 2: Measurement of Quantum and Interfacial Capacitance

To measure the capacitance between the electrolyte and the graphene, we measured the electrochemical impedance spectrum (EIS). Two setups were used both giving consistent results: a custom built electrochemical impedance spectrometer based on a lock-in amplifier and a signal generator, and a Gamry automated system (model Reference 600). The impedance of the device is measured over the frequency range of  $10^{-2} \sim 10^4$  Hz, with 7 points per decade.

Figure S3 presents a typical electrochemical impedance measurement of bare graphene in 100 mM KCl. The black line is measured data and red line is fitted data. The bare graphene capacitance is  $2 \mu\text{F}/\text{cm}^2$  that was measured in 100 mM KCl.

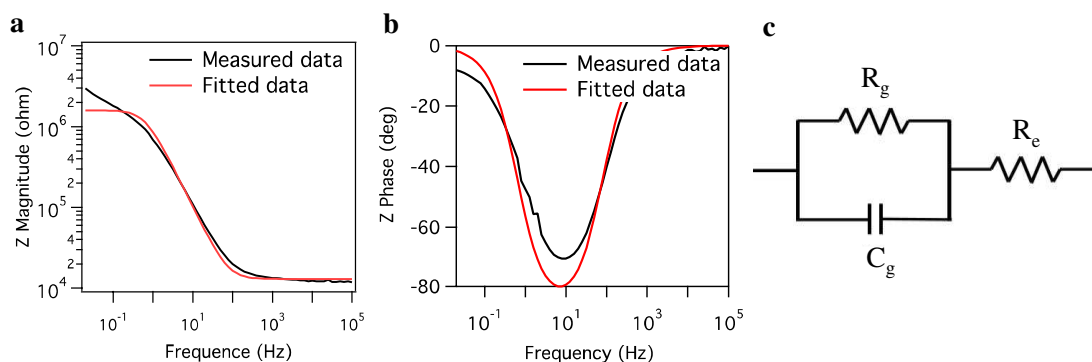


Figure S3. Electrochemical impedance measurement of bare graphene.

We performed this experiment using two different concentrations on over 20 separate devices, and present a histogram in figure S4 for the total capacitance. In the case of 1 M CsCl, the average total capacitance is  $2 \mu\text{F}/\text{cm}^2$ . In the case of 100 mM KCl, the average total capacitance is  $5 \mu\text{F}/\text{cm}^2$ . Also shown are the only other measurements in the literature,<sup>1</sup> at 0.1 and 1 mM NaF. All of the values are comparable, but there is considerable spread. It is likely

that device to device differences are due to different impurity concentrations in different devices, which are known to effect the quantum capacitance.<sup>1</sup> At present there is no theoretical explanation for the dependence of the value on the electrolyte concentration or composition, a question that is currently under investigation.

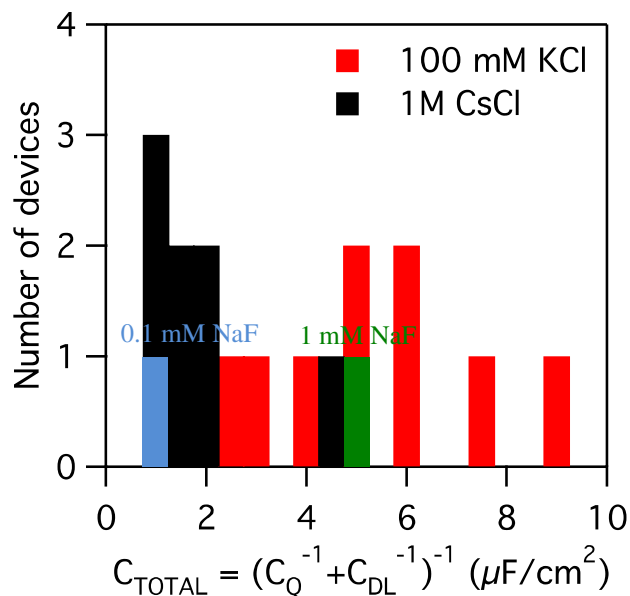


Figure S4. The number of experiment *versus* total capacitance.

In order to determine experimentally the effect that different concentrations would have on the capacitance, we measured the voltage dependent capacitance in different concentrations using the same device. The results are presented in figure S5. The voltage dependence is consistent with an impurity concentration of  $\sim 10^{12} \text{ cm}^{-2}$ , according to ref. 1.

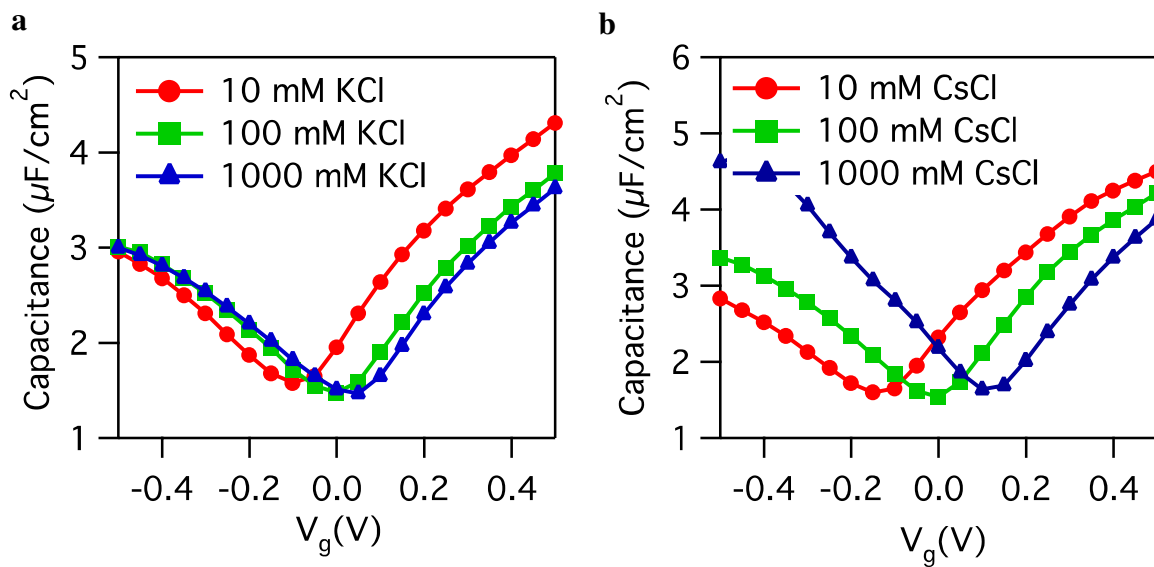


Figure S5. The capacitance as function of gate voltage in different concentration of (a) KCl and (b) CsCl.

### Supporting Information 3: Measurement of Lipid Bilayer Capacitance

To measure the lipid bilayer capacitance we next added the SLB and measured the EIS. The two time constant circuit model shown in figure S1 is used to fit experimental data. The EIS is shown in figure S6.

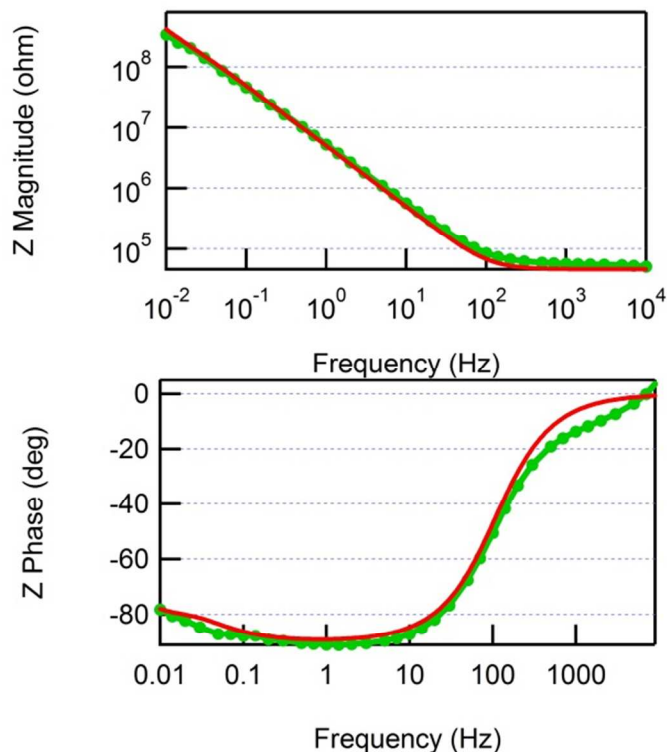


Figure S6. Measured bode plot of the device capacitance (green curve) and the curve fitted to the data (red curve).

Circuit parameters are estimated by curve fitting to the Bode plot (Figure S6). About 30% of devices have a lipid capacitance of  $0.6\text{-}0.7 \mu\text{F}/\text{cm}^2$ , which is characteristic of a lipid bilayer. For other devices the capacitance is either around  $1\text{-}1.3 \mu\text{F}/\text{cm}^2$ , showing the formation of a lipid monolayer on graphene, or around  $0.2 \mu\text{F}/\text{cm}^2$ , indicating presence of multiple lipid layers on graphene.

#### Supporting Information 4: Bilayer determination by fluorescence quenching

We developed a fluorescence based method to distinguish between bilayers, mono-bilayers and multi-bilayers. QSY-7 amine (Invitrogen, Q-10464) was used to determine whether an artificial lipid layer consists of a bilayer or otherwise.<sup>2</sup> The working principle is that QSY-7 amine can quench, *via* FRET, the fluorescence of the lipid dye reporter TexasRed DHPE (Invitrogen #T1395MP) embedded into the lipid layer. If a supported lipid bilayer is truly a bilayer, only the top layer is accessible to QSY-7 amine and therefore adding the quencher will reduce roughly half of the total fluorescence intensity. Similarly, the reduction will be less if the lipid layer is a multilayer. In our test, we fabricated SLBs on graphene as described in the method but included 0.5% mol of TexasRed DHPE for fluorescence measurement. We chose to image a field of view equivalent to 420x220  $\mu\text{m}$  at the center of the graphene device to represent the quality of the deposited bilayer (Figure S7a).

The images were taken with an inverted IX71 fluorescence microscope equipped with a broadband excitation lamp and a TRITC filter. The fluorescence intensity is measured and false colored red with Image J. After taking initial images, 2  $\mu\text{L}$  of 48  $\mu\text{M}$  QSY-7 amine was added to the bath solution and images were retaken for the same field of view after 2 min incubation (Figure S7b). Of all the devices we tested, 30% showed approximately 50% decrease in fluorescence intensity, indicating the formation of a true lipid bilayer (Figure S7c). Once we determined the bilayer nature of our supported bilayer, we proceeded to capacitance measurement of the same device.



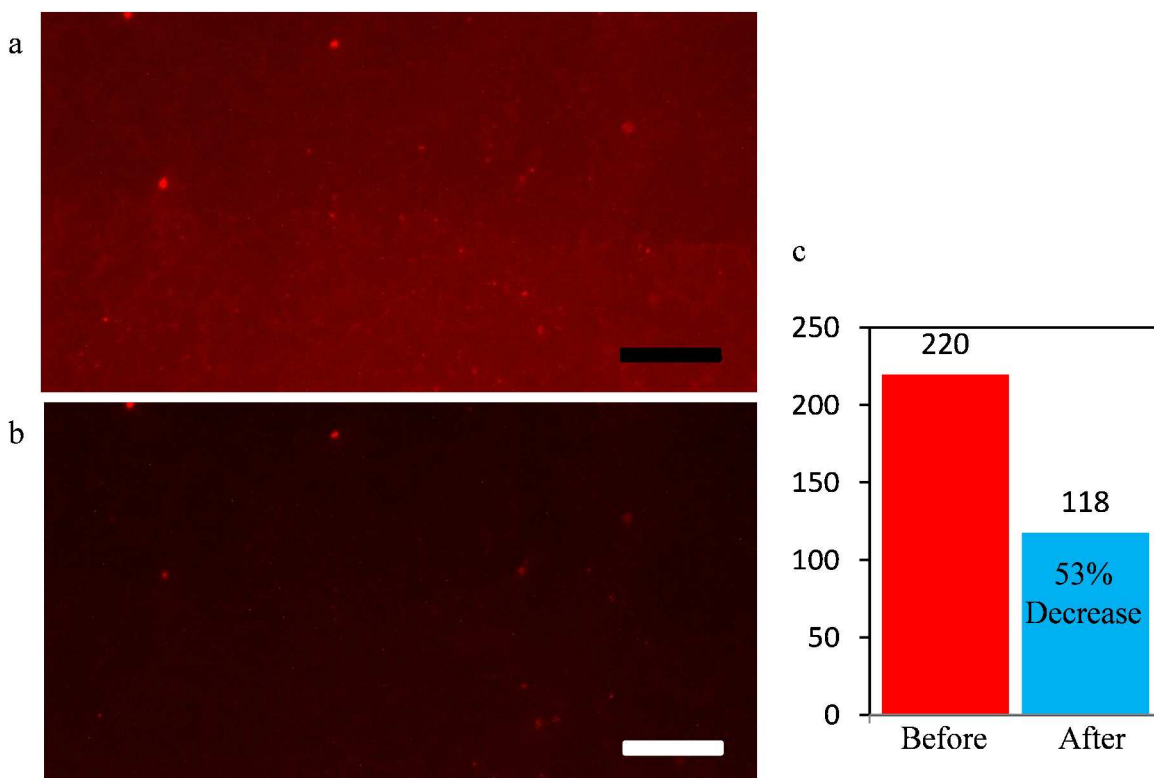


Figure S7. Images of the same field of view (a) before and (b) after adding QSY-7 amine. scale bars are 50  $\mu\text{m}$ . (c) Measured fluorescence intensity of the field of view before and after the addition of QSY-7 amine.

## Supporting Information 5: Current traces of ion channel gA at different bias

The SLBs with gA channels are deposited on graphene surface to detect single ion channel activity. The single ion channel activity is detected at the different applied potential from -100 to 100 mV (Figure S8a). In the applied voltage 100 mV, the opening and closing events are observed. The current step is about 12 pA. In the 50 mV applied potential, the ion channel activity is also observed. The current step is about 6 pA. The gA is a voltage-independent ion channel. There is no effect of voltage on closing and opening ion channel. When gA ion channel is open, the  $\text{Cs}^+$  ions can pass through from outside solution (1 M CsCl) of SLBs to inside solution water. Then the current steps are observed in the recording trace. We expect to see current steps of gA ion channel have systematic correlation with applied voltage. However, the negative current steps of gA are not observed at applied voltage -50 and -100 mV. Before the formation of SLBs, the graphene device is only soaked by distilled water overnight. Then lipid vesicles solution is added to form SLBs. The device is also rinsed by distilled water for several times. Therefore, there is only water existing on top of SLBs and between SLBs and graphene. When the ion channel measurement is conducted, the water will be replaced by 1 M CsCl solution. The SLBs is stable and continue to cover the graphene surface. The CsCl ions are not able to pass through SLBs. Therefore, only pure water exists between SLBs and graphene. When the negative voltage is applied, no CsCl ion can pass ion channel gA. Then no current steps can be observed in the negative applied voltage. The histogram of current trace at 100 mV is presented (Figure S8b). The left peak is the baseline of current trace at 0 pA. The right peak is opened ion channel at 12 pA. Figure S8c is the histogram of current trace at 50 mV. The baseline current is at 0 pA and the opened ion channel is at 6 pA.

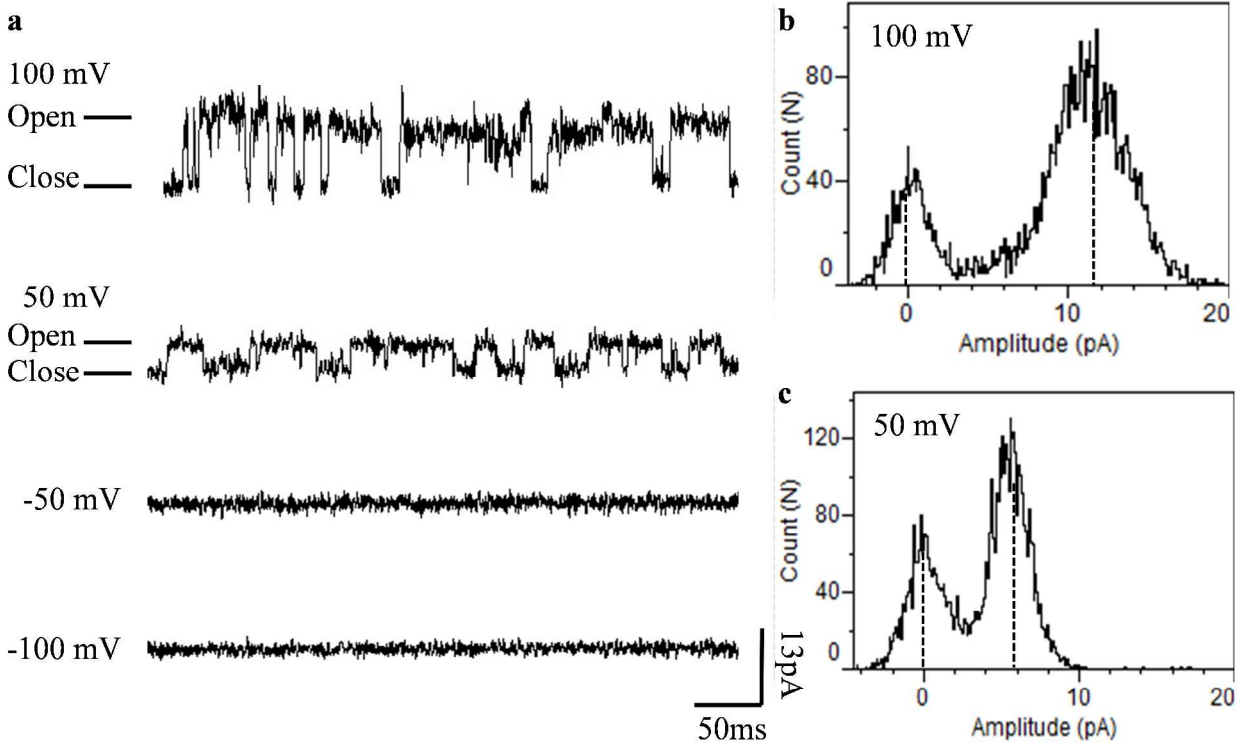


Figure S8. (a) Current traces are measured at different voltage from -100 mV to 100 mV. (b) The histogram of current trace at 100 mV. (c) The histogram of current trace at 50 mV.

### Supporting Information 6: Current traces of ion channel alamethicin at different bias

Figure S9a presents ion channel activity of alamethicin detected by graphene-SLBs devices at different applied potential from -200 to 200 mV at 0.1 M KCl solution. For 200 mV applied voltage, the current spikes of ion channel are about 120 pA. The open dwell times are from 50 to 100 ms. The second current trace is alamethicin channel activity in 100 mV applied potential. The different levels of spikes are observed. The single current of each level is about 35 pA. The open well times are from 50 to 100 ms. There is no current spike observed during the recording when the applied voltage is in both -100 and -200 mV. Because the surface of SLBs has no negative charged, the alamethicin peptides are not able to form ion channels in the SLBs. The histogram of current trace at 200 mV is showed (Figure S9b). The left peak is baseline of current trace at 0 pA. The right peak is current step at 120 pA while the ion channel is formed. Figure S9c is the histogram of current trace at 100 mV. The multi-steps of current are detected.

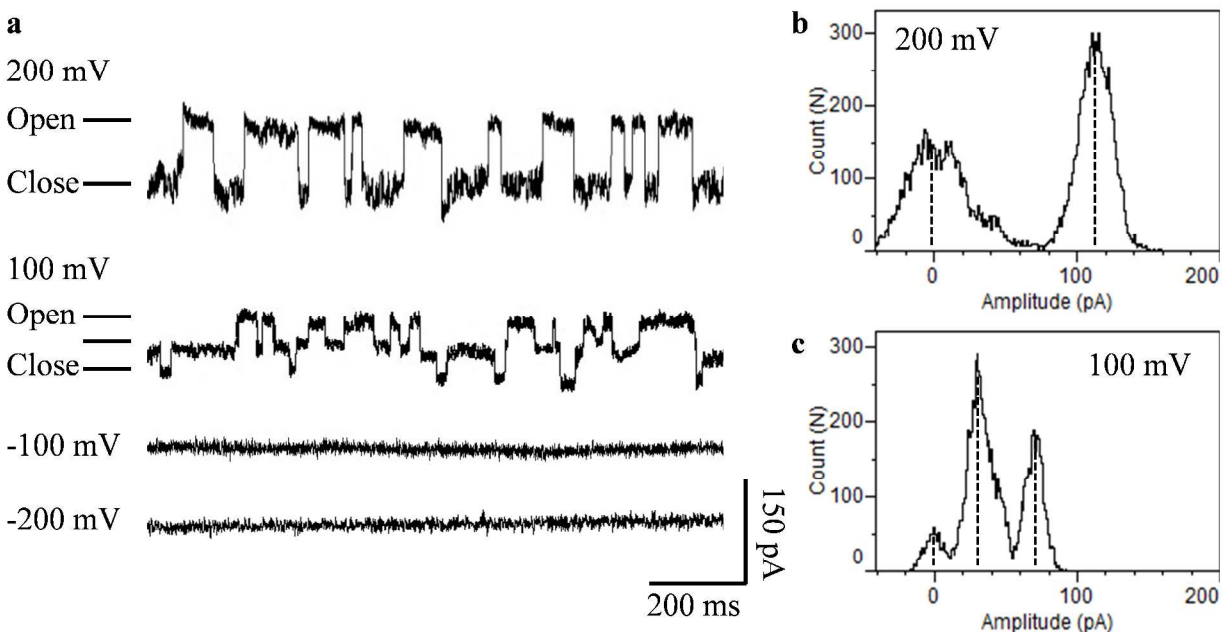


Figure S9. (a) Current traces measured at different voltage from -200 mV to 200 mV. (b) Histogram of current trace at 200 mV. (c) Histogram of current trace at 100 mV.

## Supporting Information 7: Contact angle measurement of graphene surface

(Figure S10a). After the copper foil is etched, the contact angle is still about 150° (Figure S10b). Then the graphene is soaked in DI water for overnight as the standard procedure for depositing SLBs. The graphene surface is maintained in wet condition when dropping the water. Then contact angle of drop water on graphene surface

(Figure S10c). This indicated the transformation of graphene surface from hydrophobic to hydrophilic. This is due to the adsorption of hydrophilic OH groups on graphene surface after graphene is soaked in DI water for overnight.

(Figure S10d). The graphene surface becomes hydrophobic after graphene surface is totally dry.

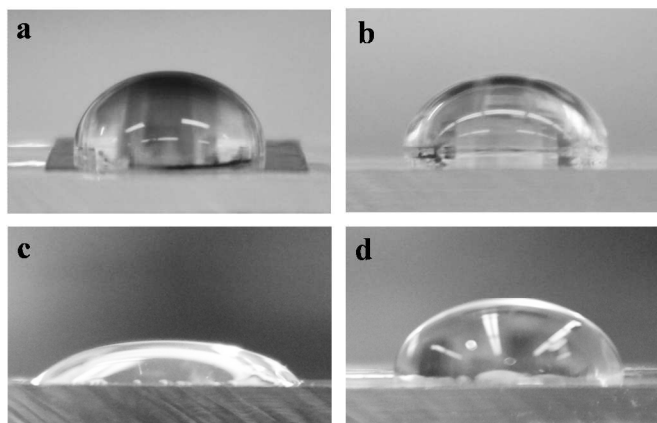


Figure S10. (a) CVD-grown graphene on copper foil. (b) Graphene is transferred on PDMS. (c) Graphene is soaked in DI water for overnight. (d) Graphene is dried for overnight.

## Supporting Information 8: Analysis of alamethicin current histogram

In order to more thoroughly analyze the conductance steps and the current level separation between peaks observed using alamethicin, we compare the spacing between peaks we observe and that of a typical value from a suspended lipid bilayer measurement of the same protein in figure S11 below. The location of the peaks we observe is consistent with those measured in the literature for the identical ion channel membrane protein.<sup>3,4</sup> (The current scale for our data is adjusted to match, as we do not know the exact value of the voltage across the bilayer in our experiments). The first two peaks (including the peak for zero current, *i.e.* a totally closed ion channel, and a barely open channel) are not resolved in our experiments. The location of the third and fourth peak relative to each other and the zero current peak are identical to that observed in the literature for alamethicin in suspended bilayers. The fifth peak is not resolved in our measurement time. This is strong evidence that we are observing the opening and closing of a single alamethicin ion channel in our SLB experiments.

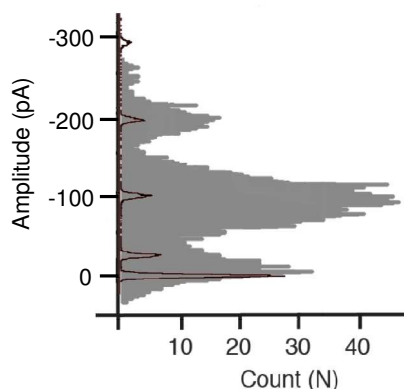


Figure S11. Ion channel current histogram of alamethicin. Grey histogram is this work. Black overlay is adapted from Ref. 4 of a suspended alamethicin showing the 4 peaks and the zero current (closed) peak. The alignment shows consistency between our measurement and suspended lipid bilayer measurements of the same ion channel.

## Supporting Information 9: Fluorescence recovery after photobleaching (FRAP) of SLBs on graphene surface

For the fluorescence recovery after photobleaching (FRAP) experiment, we deposited SLBs on graphene surface which was transferred by PMMA and annealed in Ar / H<sub>2</sub> ( 50 % / 50 % ) at 400 °C for 1 hour. Figure S12a shows fluorescence image of SLBs on graphene surface before bleached. Then the fluorescent dye at the center of red circle with radius 30 μm is bleached in figure S12b. After 18.5 minutes, the fluorescence intensity at the center of red circle is recovered as the half of initial intensity in figure S12c. Figure S12d presents that fluorescence intensity at the center of red circle recovers over time. The diffusion coefficient is 0.18 μm<sup>2</sup>/s. The calculation is using following equation  $D = 0.224 \times \omega^2/t_{1/2}$ . D is the diffusion coefficient,  $\omega$  is the radius of the photobleached spot and  $t_{1/2}$  is the time at which half of the intensity was recovered.<sup>5</sup>

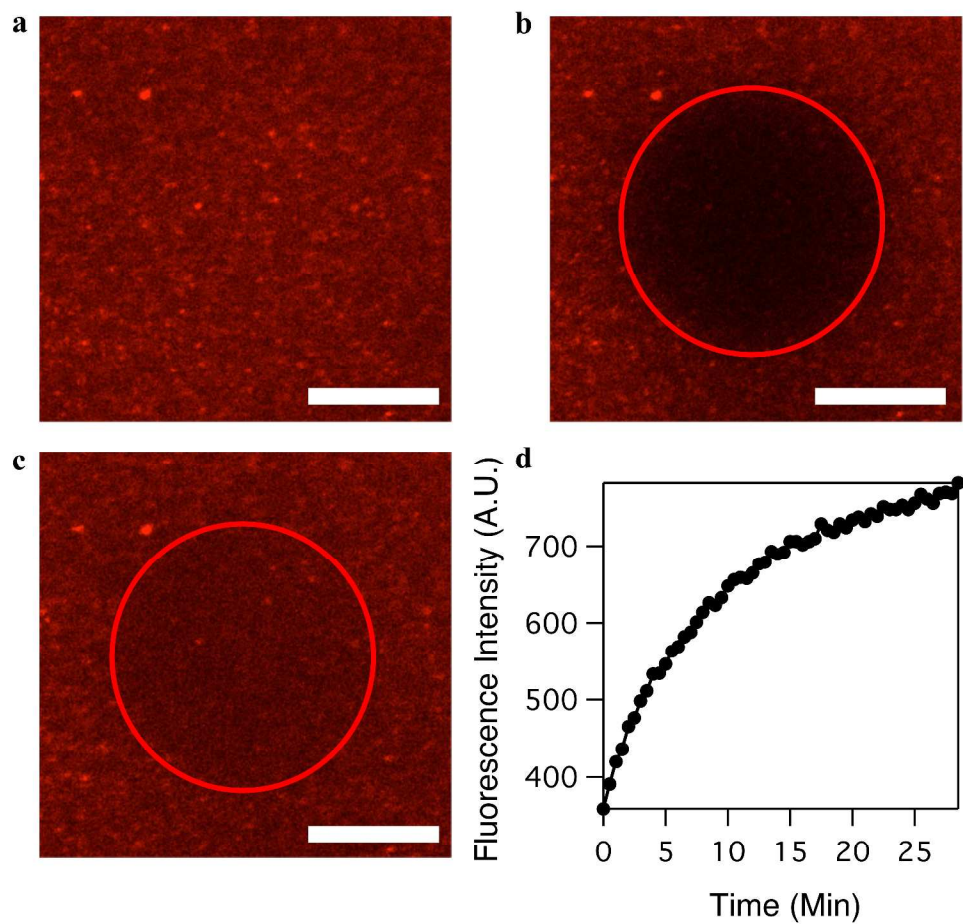


Figure S12. Fluorescence images of SLBs on graphene surface. (a) Before bleached. (b) After bleached at time 0. (c) After bleached at time 18.5 minutes. (d) Fluorescence intensity at the center of the red circle recovers over time. The scale bar is 30  $\mu\text{m}$ .



## Supporting Information 10: Atomic force microscope images of graphene and SLBs

Figure S13a is AFM image of SLBs on graphene surface. The deposition of SLBs is the same as written in the method of main paper. This image is scanned by contact-mode AFM in water. The SLBs presents uniformly and completely covering graphene surface. The z-axis scale bar is from 0 to 16 nm. Figure S13b presents the SLBs' height histogram of scanned area figure (a). The height difference from the lowest point to highest point is less than 5 nm. The result shows that the surface of SLBs is very smooth and uniform.

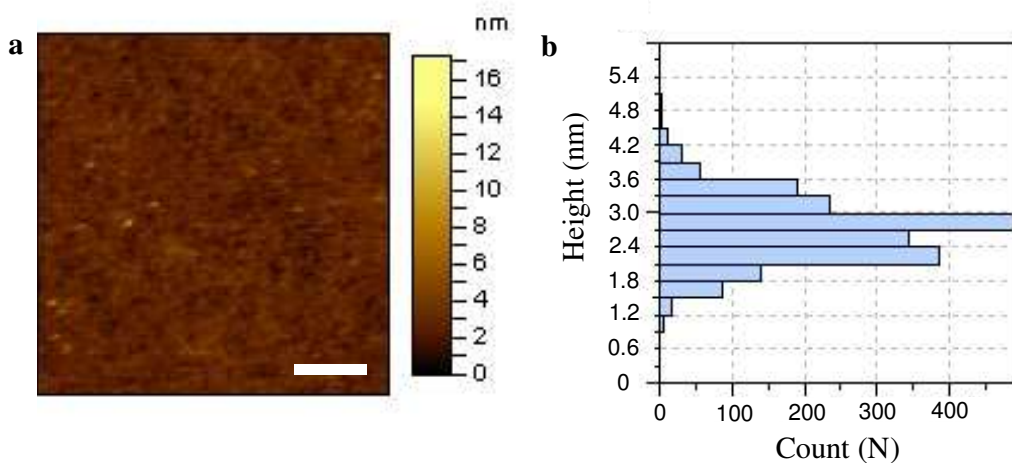


Figure S13. Atomic force microscope images. (a) SLBs on graphene surface taken by contact-mode AFM in water. The scale bar is 1  $\mu\text{m}$ . (b) The SLBs' height histogram of scanned area figure (a).

## Supporting Information 11: Yield and statistics

We conducted 16 separate experiments to measure the ion channel current through gA, and varied the starting gA concentration between 0.1 and 10 mM. In each experiment we recorded at least 30 current vs. time traces at different bias voltages. The ion channel open and close events were observed for least 2 current traces for concentrations of 1, 2 and 10 mM gA. The ion channel open and close events were observed in 12 current traces for 0.1 mM gA. Similarly, the ion channel alamethicin experiments were performed 6 times. At least 30 current traces will be recorded in each experiment. We observed 6 current traces with ion channel open and close events. Although we have not done a systematic study, this yield seems to improve with lower applied lower voltages across the lipid bilayer. At voltages larger than 0.5 V, this yield drops to zero. This is consistent with the known properties of both suspended and supported lipid bilayers.

For electrochemical impedance measurements, we conducted 14 separate experiments. In 4 of these experiments the capacitance indicated the presence of a lipid bilayer (not multilayer and not monolayer). For these, the average capacitance of SLBs is  $0.63 \pm 0.09 \mu\text{F}/\text{cm}^2$ . For AFM measurement of SLBs on the graphene surface, 3 experiments were performed. All AFM images showed uniform SLBs on the graphene surface. For FRAP measurements, 4 experiments were conducted, with qualitatively similar results for each FRAP experiment indicating that the lipids were free to diffuse as expected, and consistent with ref. 6.

## References

1. Xia, J.; Chen, F.; Li, J.; Tao, N. Measurement of the Quantum Capacitance of Graphene. *Nat. Nanotechnol.* **2009**, *4*, 505–509.
2. Freeman, L. M.; Li, S.; Dayani, Y.; Choi, H.-S.; Malmstadt, N.; Armani, A. M. Excitation of Cy5 in Self-assembled Lipid Bilayers Using Optical Microresonators. *Appl. Phys. Lett.* **2011**, *98*, 143703.
3. Andrew Woolley, G.; Wallace, B. A. Model Ion Channels: Gramicidin and Alamethicin. *J. Membr. Biol.* **1992**, *129*, 109–136.
4. Baaken, G.; Sondermann, M.; Schlemmer, C.; Rühle, J.; Behrends, J. C. Planar Microelectrode-Cavity Array for High-Resolution and Parallel Electrical Recording of Membrane Ionic Currents. *Lab Chip* **2008**, *8*, 938.
5. Nirasay, S.; Badia, A.; Leclair, G.; Claverie, J.; Marcotte, I. Polydopamine-Supported Lipid Bilayers. *Materials*. **2012**, *5*, 2621–2636.
6. Ang, P. K.; Jaiswal, M.; Lim, C. H. Y. X.; Wang, Y.; Sankaran, J.; Li, A.; Lim, C. T.; Wohland, T.; Barbaros, Ö.; Loh, K. P. A Bioelectronic Platform Using a Graphene-Lipid Bilayer Interface. *ACS Nano* **2010**, *4*, 7387–7394.